Data sources for Figure 1

Ultramafic Xenoliths

Europe

Ackerman et al. (2009)	Czech Republic
Harvey et al. (2010)	Massif Central, France
Choi et al. (2010)	Spitsbergen
Alard et al. (2011)	Montferrier, France

Asia

Gao et al. (2002)	Hannuoba
Wu et al. (2003)	NE China
Pearson et al. (2004)	Vitim, Siberia
Reisberg et al. (2005)	Eastern China
Wu et al. (2006)	NE China
Lee and Walker (2006)	South Korea
Xu et al. (2008)	Western China
Zhang HF et al. (2008)	South China Craton
Chu et al. (2009)	Eastern China
Zhang HF et al. (2009)	Hannuoba
Yang et al. (2010)	North Korea
Liu J et al. (2010)	Trans N. China Orogen
Liu J et al. (2011)	North China craton
Zhang YL et al. (2011)	CAOB, NE China
Zhang M et al. (2012)	Eastern central CAOB
Zhang HF et al. (2012)	Western NCC
Yu et al (2012)	NE China
Hong et al. (2012)	NE China
Liu CZ et al. (2012a)	S China
Liu CZ et al. (2012b)	SE China
Sun et al. (2012)	North China craton
Liu CZ et al. (2013)	SW China
Chen et al. (2014)	NW China, Tarim Block

N. America

Lee et al. (2000)	Sierra Nevada
Peslier et al. (2000a)	Canadian Cordillera
Peslier et al. (2000b)	Canadian Cordillera
Harvey et al. (2011)	Kilbourne Hole
Byerly and Lassiter (2012)	Rio Grande Rift
Armytage et al. (2014)	Dish Hill, California

Africa

Reisberg et al. (2004)	Sidamo East Africa
Wittig et al. (2010)	Morocco

Australia

McBride et al. (1996)	SE Australia
Handler et al. (1997)	SE Australia
Handler et al. (2005)	N. Queensland, Australia

Antarctica

Handler et al. (2003)	W. Antarctica

Various

Meisel et al. (2001)	Mexico, Pacific, Europe, Asia
Becker et al. (2006)	Kilbourne Hole, San Carlos, San Quintin, Labait, Matsoku, Hannuoba, Mt. Quincan
Fischer-Gödde et al. (2011)	Hannuoba, West Eifel

Orogenic Peridotites

Reisberg et al. (1991)	Ronda, Spain
Reisberg and Lorand (1995)	E. Pyrenees, France
Snow et al. (2000)	External Ligurgides, Italy
Saal et al. (2001)	Horoman, Japan
Pearson et al. (2004)	Beni Bousera, Morocco
Becker et al. (2006)	Various
Riches and Rogers (2011)	Lherz, France
Fischer-Gödde et al. (2011)	Various
Wang et al. (2013)	Balmuccia, Baldissero, Italy

References

Ackerman, L., Walker, R.J., Puchtel, I.S., Pitcher, L., Jelínek, E., Strnad, L., 2009. Effects of melt percolation on highly siderophile elements and Os isotopes in subcontinental lithospheric mantle: A study of the upper mantle profile beneath Central Europe. Geochimica et Cosmochimica Acta 73, 2400–2414. https://doi.org/10.1016/j.gca.2009.02.002

Alard, O., Lorand, J.-P., Reisberg, L., Bodinier, J.-L., Dautria, J.-M., O'Reilly, S.Y., 2011. Volatile-rich Metasomatism in Montferrier Xenoliths (Southern France): Implications for the Abundances of Chalcophile and Highly Siderophile Elements in the Subcontinental Mantle. J Petrology 52, 2009–2045. https://doi.org/10.1093/petrology/egr038

Armytage, R.M.G., Brandon, A.D., Peslier, A.H., Lapen, T.J., 2014. Osmium isotope evidence for Early to Middle Proterozoic mantle lithosphere stabilization and concomitant production of juvenile crust in Dish Hill, CA peridotite xenoliths. Geochimica et Cosmochimica Acta 137, 113–133. https://doi.org/10.1016/j.gca.2014.04.017

Becker, H., Horan, M.F., Walker, R.J., Gao, S., Lorand, J.-P., Rudnick, R.L., 2006. Highly siderophile element compositions of the earth's primitive mantle. Geochim. Cosmochim. Acta 70, 4528–4550.

Byerly, B.L., Lassiter, J.C., 2012. Evidence from mantle xenoliths for lithosphere removal beneath the central Rio Grande Rift. Earth and Planetary Science Letters 355–356, 82–93. https://doi.org/10.1016/j.epsl.2012.08.034

Chen, M.-M., Tian, W., Suzuki, K., Tejada, M.-L.-G., Liu, F.-L., Senda, R., Wei, C.-J., Chen, B., Chu, Z.-Y., 2014. Peridotite and pyroxenite xenoliths from Tarim, NW China: Evidences for melt depletion and mantle refertilization in the mantle source region of the Tarim flood basalt. Lithos, Special Issue Permian large igneous provinces: Characteristics, mineralization and paleo-environment effects 204, 97–111. https://doi.org/10.1016/j.lithos.2014.01.005

Choi, S.H., Suzuki, K., Mukasa, S.B., Lee, J.-I., Jung, H., 2010. Lu–Hf and Re–Os systematics of peridotite xenoliths from Spitsbergen, western Svalbard: Implications for mantle–crust coupling. Earth and Planetary Science Letters 297, 121–132. https://doi.org/10.1016/j.epsl.2010.06.013

Chu, Z.-Y., Wu, F.-Y., Walker, R.J., Rudnick, R.L., Pitcher, L., Puchtel, I.S., Yang, Y.-H., Wilde, S.A., 2009. Temporal Evolution of the Lithospheric Mantle beneath the Eastern North China Craton. J. Petrol. 50, 1857–1898. https://doi.org/10.1093/petrology/egp055

Fischer-Gödde, M., Becker, H., Wombacher, F., 2011. Rhodium, gold and other highly siderophile elements in orogenic peridotites and peridotite xenoliths. Chemical Geology 280, 365–383. https://doi.org/10.1016/j.chemgeo.2010.11.024

Handler, M.R., Bennett, V.C., Carlson, R.W., 2005. Nd, Sr and Os isotope systematics in young, fertile spinel peridotite xenoliths from northern Queensland, Australia: A unique view of depleted MORB mantle? Geochimica et Cosmochimica Acta 69, 5747–5763. https://doi.org/10.1016/j.gca.2005.08.003

Handler, M.R., Bennett, V.C., Esat, T.M., 1997. The persistence of off-cratonic lithospheric mantle: Os isotopic systematics of variably metasomatised southeast Australian xenoliths. Earth Planet. Sci. Lett. 151, 61–75.

Handler, M.R., Wysoczanski, R.J., Gamble, J.A., 2003. Proterozoic lithosphere in Marie Byrd Land, West Antarctica: Re–Os systematics of spinel peridotite xenoliths. Chemical Geology, Highly Siderophile elements in the Earth and Meteorties: A volume in honor of john Morgan 196, 131–145. https://doi.org/10.1016/S0009-2541(02)00410-2

Harvey, J., Dale, C.W., Gannoun, A., Burton, K.W., 2011. Osmium mass balance in peridotite and the effects of mantle-derived sulphides on basalt petrogenesis. Geochim. Cosmochim. Acta 75, 5574–5596. https://doi.org/10.1016/j.gca.2011.07.001

Harvey, J., Gannoun, A., Burton, K.W., Schiano, P., Rogers, N.W., Alard, O., 2010. Unravelling the effects of melt depletion and secondary infiltration on mantle Re–Os isotopes beneath the French Massif Central. Geochimica et Cosmochimica Acta 74, 293–320. https://doi.org/10.1016/j.gca.2009.09.031

Hong, L.-B., Xu, Y.-G., Ren, Z.-Y., Kuang, Y.-S., Zhang, Y.-L., Li, J., Wang, F.-Y., Zhang, H., 2012. Petrology, geochemistry and Re-Os isotopes of peridotite xenoliths from Yantai, Shandong Province: Evidence for Phanerozoic lithospheric mantle beneath eastern North China Craton. Lithos 155, 256–271. https://doi.org/10.1016/j.lithos.2012.09.005

Lee, C.-T., Yin, Q., Rudnick, R.L., Chesley, J.T., Jacobsen, S.B., 2000. Osmium Isotopic Evidence for Mesozoic Removal of Lithospheric Mantle Beneath the Sierra Nevada, California. Science 289, 1912–1916. https://doi.org/10.1126/science.289.5486.1912

Lee, S.R., Walker, R.J., 2006. Re-Os isotope systematics of mantle xenoliths from South Korea: evidence for complex growth and loss of lithospheric mantle beneath East Asia. Chem. Geol. 231, 90–101.

Liu, C.-Z., Liu, Z.-C., Wu, F.-Y., Chu, Z.-Y., 2012a. Mesozoic accretion of juvenile sub-continental lithospheric mantle beneath South China and its implications: Geochemical and Re-Os isotopic results from Ningyuan mantle xenoliths. Chem. Geol. 291, 186–198. https://doi.org/10.1016/j.chemgeo.2011.10.006

Liu, C.-Z., Wu, F.-Y., Sun, J., Chu, Z.-Y., Qiu, Z.-L., 2012b. The Xinchang peridotite xenoliths reveal mantle replacement and accretion in southeastern China. Lithos 150, 171–187. https://doi.org/10.1016/j.lithos.2012.03.019

Liu, C.-Z., Wu, F.-Y., Sun, J., Chu, Z.-Y., Yu, X.-H., 2013. Petrology, geochemistry and Re-Os isotopes of peridotite xenoliths from Maguan, Yunnan Province: Implications for the Cenozoic mantle replacement in southwestern China. Lithos 168, 1–14. https://doi.org/10.1016/j.lithos.2013.01.011

Liu, J., Rudnick, R.L., Walker, R.J., Gao, S., Wu, F., Piccoli, P.M., 2010. Processes controlling highly siderophile element fractionations in xenolithic peridotites and their influence on Os isotopes. Earth Planet. Sci. Lett. 297, 287–297. https://doi.org/10.1016/j.epsl.2010.06.030

Liu, J., Rudnick, R.L., Walker, R.J., Gao, S., Wu, F., Piccoli, P.M., Yuan, H., Xu, W., Xu, Y.-G., 2011. Mapping lithospheric boundaries using Os isotopes of mantle xenoliths: An example from the North China Craton. Geochim. Cosmochim. Acta 75, 3881–3902. https://doi.org/10.1016/j.gca.2011.04.018

McBride, J.S., Lambert, D.D., Greig, A., Nicholls, I.A., 1996. Multistage evolution of Australian subcontinental mantle: Re-Os isotopic constraints from Victorian mantle xenoliths. Geology 24, 631–634.

Meisel, T., Walker, R.J., Irving, A.J., Lorand, J.-P., 2001. Osmium isotopic compositions of mantle xenoliths: a global perspective. Geochim. Cosmochim. Acta. 65, 1311–1323.

Pearson, D.G., Irvine, G.J., Ionov, D.A., Boyd, F.R., Dreibus, G.E., 2004. Re-Os isotope systematics and platinum group element fractionation during mantle melt extraction: a study of massif and xenolith peridotite suites. Chem. Geol. 208, 29–59.

Peslier, A., Reisberg, L., Ludden, J., Francis, D., 2000. Os isotopic systematics in mantle xenoliths; age constraints on the Canadian Cordillera lithosphere. Chem. Geol. 166, 85–101.

Peslier, A.H., Reisberg, L., Ludden, J., Francis, D., 2000. Re-Os constraints on harzburgite and lherzolite formation in the lithospheric mantle: A study of Northern Canadian Cordillera xenoliths. Geochim. Cosmochim. Acta 64, 3061–3071.

Reisberg, L., Lorand, J.-P., 1995. Longevity of sub-continental mantle lithosphere from osmium isotope systematics in orogenic peridotite massifs. Nature 376, 159–162.

Reisberg, L., Lorand, J.-P., Bedini, R.M., 2004. Reliability of Os model ages in pervasively metasomatized continental mantle lithosphere: a case study of Sidamo spinel peridotite xenoliths (East African Rift, Ethiopia). Chem. Geol. 208, 119–140.

Reisberg, L., Zhi, X., Lorand, J.-P., Wagner, C., Peng, Z., Zimmermann, C., 2005. Re-Os and S systematics of spinel peridotite xenoliths from east central China: Evidence for contrasting effects of melt percolation. Earth Planet. Sci. Lett. 239, 286–308.

Reisberg, L.C., Allègre, C.-J., Luck, J.-M., 1991. The Re-Os systematics of the Ronda Ultramafic Complex of southern Spain. Earth Planet. Sci. Lett. 105, 196–213.

Riches, A.J.V., Rogers, N.W., 2011. Mineralogical and geochemical constraints on the shallow origin, ancient veining, and multi-stage modification of the Lherz peridotite. Geochimica et Cosmochimica Acta 75, 6160–6182. https://doi.org/10.1016/j.gca.2011.07.036

S. Gao, R. Rudnick, R. W. Carlson, W. F. McDonough, Y-S. Liu, 2002. Re-Os evidence for replacement of ancient mantle lithosphere beneath the North China craton. Earth Planet. Sci. Lett. 198, 307–322.

Saal, A.E., Takazawa, E., Frey, F.A., Shimizu, N., Hart, S.R., 2001. Re-Os Isotopes in the Horoman Peridotite: Evidence for Refertilization? J. Petrol. 42, 25–37.

Snow, J.E., Schmidt, G., Rampone, E., 2000. Os isotopes and highly siderophile elements (HSE) in the Ligurian ophiolites, Italy. Earth Planet. Sci. Lett. 175, 119–132.

Sun, J., Liu, C.-Z., Wu, F.-Y., Yang, Y.-H., Chu, Z.-Y., 2012. Metasomatic origin of clinopyroxene in Archean mantle xenoliths from Hebi, North China Craton: Trace-element and Sr-isotope constraints. Chem. Geol. 328, 123–136. https://doi.org/10.1016/j.chemgeo.2012.03.014

Wang, Z., Becker, H., Gawronski, T., 2013. Partial re-equilibration of highly siderophile elements and the chalcogens in the mantle: A case study on the Baldissero and Balmuccia peridotite massifs (Ivrea Zone, Italian Alps). Geochim. Cosmochim. Acta 108, 21–44. https://doi.org/10.1016/j.gca.2013.01.021

Wittig, N., Pearson, D.G., Baker, J.A., Duggen, S., Hoernle, K., 2010. A major element, PGE and Re–Os isotope study of Middle Atlas (Morocco) peridotite xenoliths: Evidence for coupled introduction of metasomatic sulphides and clinopyroxene. Lithos 115, 15–26. https://doi.org/10.1016/j.lithos.2009.11.003

Wu F. Y, Walker R. J, Ren X. W, Sun D. Y, Zhou X. H, 2003. Osmium isotopic constraints on the age of lithospheric mantle beneath northeastern China. Chem. Geol. 196, 107–129.

Wu, F.-Y., Walker, R.J., Yang, Y.-H., Yuan, H.-L., Yang, J.-H., 2006. The chemical-temporal evolution of lithospheric mantle underlying the North China Craton. Geochim. Cosmochim. Acta 70, 5013–5034.

Xu, Y.-G., Blusztajn, J., Ma, J.-L., Suzuki, K., Liu, J.-F., Hart, S.R., 2008. Late Archean to Early Proterozoic lithospheric mantle beneath the western North China craton: Sr–Nd–Os isotopes of peridotite xenoliths from Yangyuan and Fansi. Lithos, Continental Volcanism and the Chemistry of the Earth's Interior 102, 25–42. https://doi.org/10.1016/j.lithos.2007.04.005

Yang, J.-H., O'Reilly, S., Walker, R.J., Griffin, W., Wu, F.-Y., Zhang, M., Pearson, N., 2010. Diachronous decratonization of the Sino-Korean craton: Geochemistry of mantle xenoliths from North Korea. Geology 38, 799–802. https://doi.org/10.1130/G30944.1

Yu, S., Song, X., Xu, Y., Chen, L., Li, J., 2012. Effects of melt percolation on the Re-Os systematics of continental mantle lithosphere: A case study of spinel peridotite xenoliths from Heilongjiang, NE China. Sci. China-Earth Sci. 55, 949–965. https://doi.org/10.1007/s11430-012-4372-9

Zhang, H.-F., Goldstein, S.L., Zhou, X.-H., Sun, M., Cai, Y., 2009. Comprehensive refertilization of lithospheric mantle beneath the North China Craton: further Os-Sr-Nd isotopic constraints. J. Geol. Soc. 166, 249–259. https://doi.org/10.1144/0016-76492007-152

Zhang, H.-F., Goldstein, S.L., Zhou, X.-H., Sun, M., Zheng, J.-P., Cai, Y., 2008. Evolution of subcontinental lithospheric mantle beneath eastern China: Re-Os isotopic evidence from mantle xenoliths in Paleozoic kimberlites and Mesozoic basalts. Contrib. Mineral. Petrol. 155, 271–293. https://doi.org/10.1007/s00410-007-0241-5

Zhang, H.-F., Sun, Y.-L., Tang, Y.-J., Xiao, Y., Zhang, W.-H., Zhao, X.-M., Santosh, M., Menzies, M.A., 2012. Melt-peridotite interaction in the Pre-Cambrian mantle beneath the western North China Craton: Petrology, geochemistry and Sr, Nd and Re isotopes. Lithos 149, 100–114. https://doi.org/10.1016/j.lithos.2012.01.027

Zhang, M., Yang, J.-H., Sun, J.-F., Wu, F.-Y., Zhang, Ming, 2012. Juvenile subcontinental lithospheric mantle beneath the eastern part of the Central Asian Orogenic Belt. Chem. Geol. 328, 109–122. https://doi.org/10.1016/j.chemgeo.2012.07.010

Zhang, Y.-L., Liu, C.-Z., Ge, W.-C., Wu, F.-Y., Chu, Z.-Y., 2011. Ancient sub-continental lithospheric mantle (SCLM) beneath the eastern part of the Central Asian Orogenic Belt (CAOB): Implications for crust-mantle decoupling. Lithos 126, 233–247. https://doi.org/10.1016/j.lithos.2011.07.022

Melt percolation model

Mafic melts are assumed to migrate upwards in a column composed of depleted harzburgite in the cooling lithosphere. The harzburgite is assumed to have a uniform $^{187}Os/^{188}Os$ composition (on the whole rock scale), corresponding to the value of the Primitive Upper Mantle (PUM) at the time the harzburgites formed by melt extraction. The column is composed of steps of the same height. It is assumed that each increment of melt addition will create the same porosity in the bottommost step. Melt addition proceeds in the following fashion:

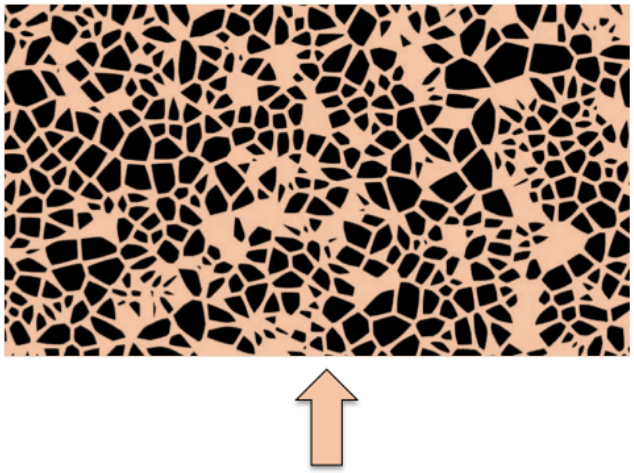

Magma (beige) from underlying asthenosphere enters lowest step of column. Amount of magma exaggerated for illustration.

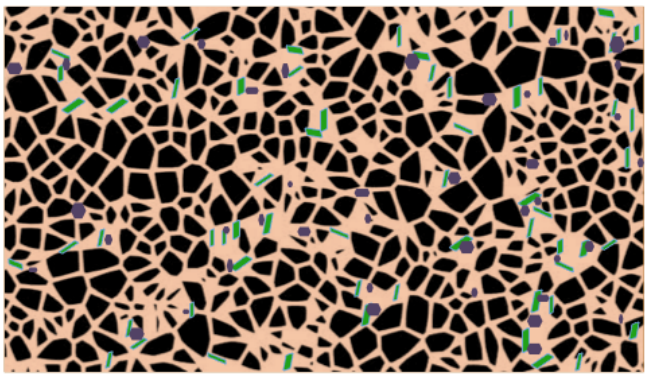

Pyroxene (green) and spinel/garnet (purple) crystallize to an assumed fraction, decreasing volume of magma and thus increasing its sulfur concentration.

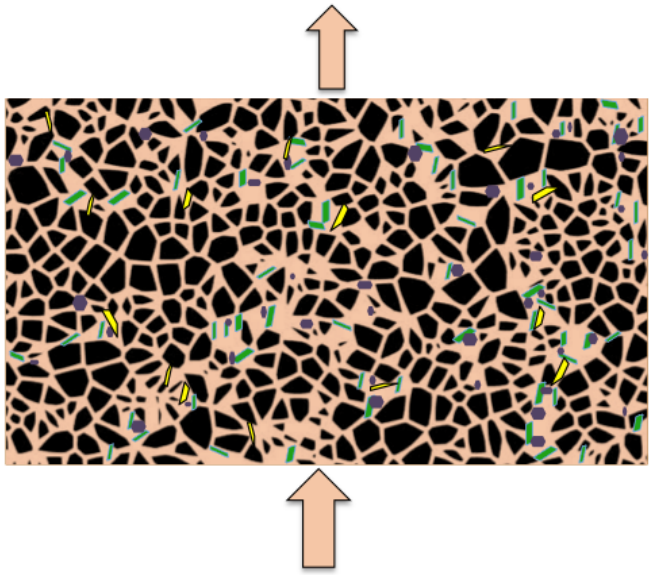

When sulfur concentration exceeds the SCSS, an immiscible sulfide liquid (yellow) forms. Re and Os requilibrate between the sulfide liquid, silicate magma and solid phases. The remaining silicate magma migrates upward into the overlying column step, and new liquid is added from below.

For simplicity, the Al_2O_3 content of the ascending silicate melt is assumed to remain constant, and the modal proportions of spinel and pyroxene are adjusted to ensure that this is the case. In the main model, in each step, reequilibration is assumed to occur only between the sulfide and silicate liquids and the newly formed phases, as bulk rock equilibration is likely to be much slower than the time scale of magma ascent. This assumption will have very little effect on the results as the Os and Re partition coefficients for opx and olivine, the main harzburgite phases, are quite low (though poorly constrained) relative to those in sulfide. This assumption was shown to be valid through development of a full equilibrium model (see text).

Input parameters used (ranges tested in parentheses):

SCSS	1000 ppm (800 - 1200 ppm)
Initial porosity bottom step	0.01 (0.002 - 0.02)
Crystallization fraction	0.1 (0.02-0.2)
[Os] initial silicate liquid	0.2 ppb (0.02-1 ppb)
[Re] initial silicate liquid	1 ppb (0.7 - 1.3 ppb)
[Os] initial peridotite	3.5 ppb (3.0 - 5.0 ppb)
[Re] initial peridotite	0.01 ppb (0 - 0.05 ppb)
$^{187}Os/^{188}Os$ liquid	0.15 (for mixing and recent melt percolation tests)
T_{RD} age most depleted sample	1.7 Ga for Lianshan samples
$D_{Os}^{sulf/sil}$	1000000 (1 - 1000000)
$D_{Re}^{sulf/sil}$	380 (40 - 40000)
Number of melt passages	320 (50 - 500)
Initial opx abundance	0.3
Initial olivine abundance	0.7
Assumed Al_2O_3 cpx	0.07 (g/g)
Assumed Al_2O_3 spinel	0.55
Assumed Al_2O_3 opx	0.06
Assumed Al_2O_3 olivine	0.001
Assumed Al_2O_3 garnet	0.2
Assumed Al_2O_3 silicate liquid	0.16 (0.14 - 0.17)
Assumed initial Al_2O_3 peridotite	0.007
K_d Os cpx	0.5 (0.001 - 10)
K_d Os spinel	90 (0.2 - 2000)
K_d Os opx	0.5
K_d Os olivine	2
K_d Os garnet	0.2 (no data - just a guess)
K_d Re cpx	0.09 (0.01 - 1)
K_d Re spinel	0.03 (0.001 - 0.2)
K_d Re opx	0.03
K_d Re olivine	0.01
K_d Re garnet	0.1 (0.01 - 1)
K_d Lu cpx	0.28
K_d Lu spinel	0.1
K_d Lu opx	0.06
K_d Lu olivine	0. 0015
K_d Lu garnet	5.5

Initial [Lu] liquid	0.3 ppm
Initial [Lu] peridotite	0.003 ppm
[Os]init liq (ppb)	0.5 (1st mixing curve)
[Os]init liq (ppb)	0.05 (2nd mixing curve)

$D_{Os}^{sulf/sil}$ based on Mungall and Brenan (2014). $D_{Re}^{sulf/sil}$ represents lower limit of range proposed by Brenan (2008); see text for discussion. K_d (Os) for silicate phases and spinel are from compilation in Brenan et al. (2016) where available; for olivine K_d is based on values of closely related elements Ir and Ru. K_d values for Re for non sulfide phases are from Mallmann and O'Neill (2007), assuming delta log fO_2 (QFM) ~0. Lu partition coefficients are from MacKenzie and O'Nions (1991) and are consistent most other values in the GERM database.

The Al_2O_3 content of the harzburgite prior to melt percolation is taken to be 0.7%. For the case of recent melt percolation, the melt is taken to have a $^{187}Os/^{188}Os$ ratio of 0.15 in the tests shown below. For the case of $^{187}Os/^{188}Os$ ratios developed through radiogenic increase, the T_{RD} age of the least radiogenic harzburgite (1.7 Ga in the example of Lianshan) is used to calculate the PUM value at the time of melting, which is assumed to be indistinguishable from the time of melt percolation.

Modal variations with height in column

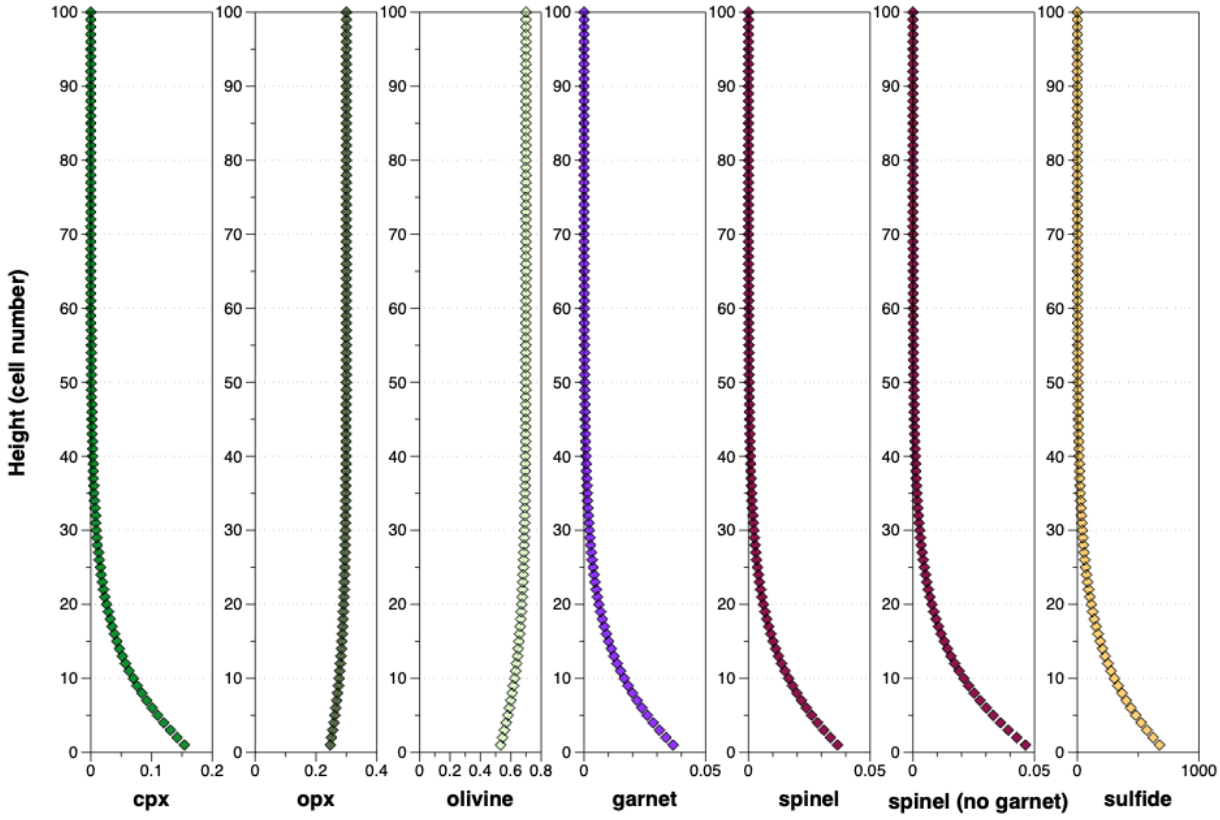

This figure shows how modal abundances vary with height in the column using the parameters given above. Two cases are shown for spinel. In the first, spinel and garnet precipitate in equal proportions from the melt percolation. In the second, spinel is the only Al_2O_3 bearing phase. Sulfide modal abundances are calculated from sulfur abundances, assuming that the sulfide composition is approximately FeS.

Parameter tests

The sensitivity of the results to the parameter choices was tested by varying each parameter individually. Results for SCSS, initial melt fraction, and $D_{Re}^{sulf/sil}$ are presented in the main text. Results for most other parameters are presented below. In all cases, results for the most likely value are shown in the left column. These choices are based on the measured partition coefficients in the references cited above, not on the values that best fit the data. The right two columns show the relationships obtained using the endmember values of a geologically reasonable range of variation (except in the case of $D_{Os}^{sulf/sil}$ where the middle column shows an intermediate value).

Effects of varying partition coefficients

Changes in the Os partition coefficients have almost no effect on the observed trends. Changes in the Re partition coefficients of the silicate and oxide phases have minor effects, but much smaller than those related to changes in $D_{Re}^{sulf/sil}$ as discussed in the main text.

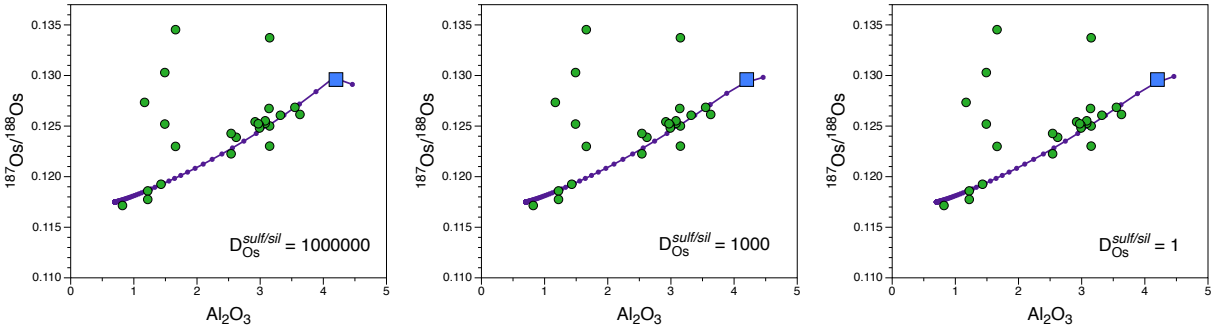

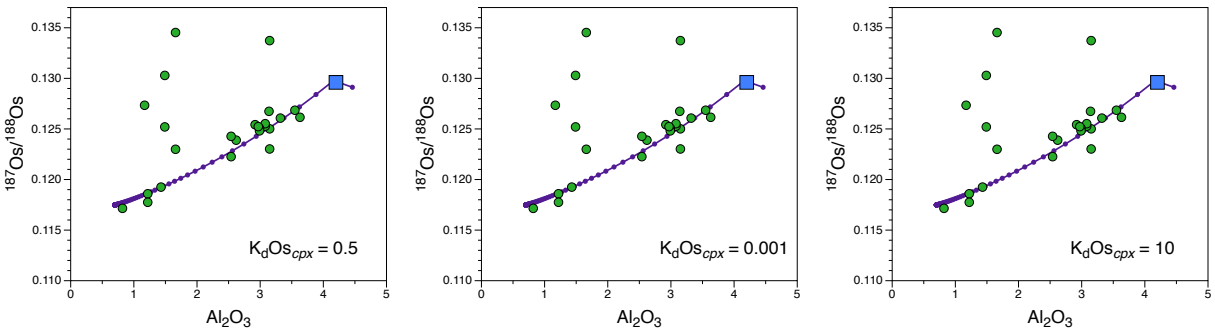

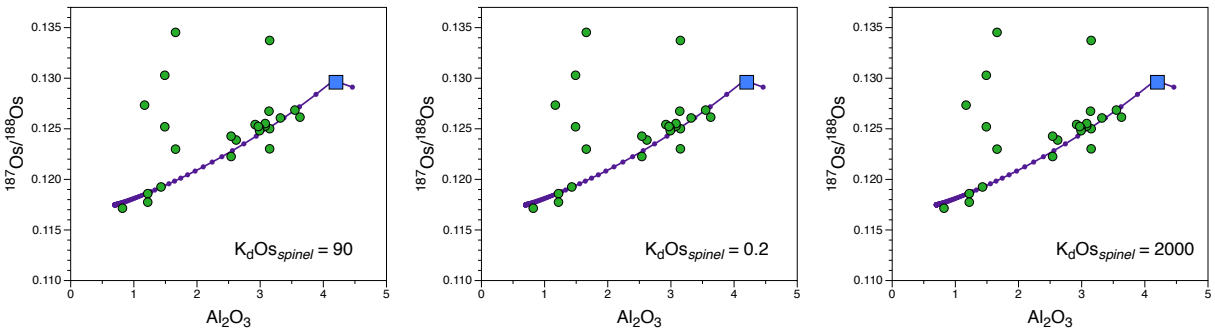

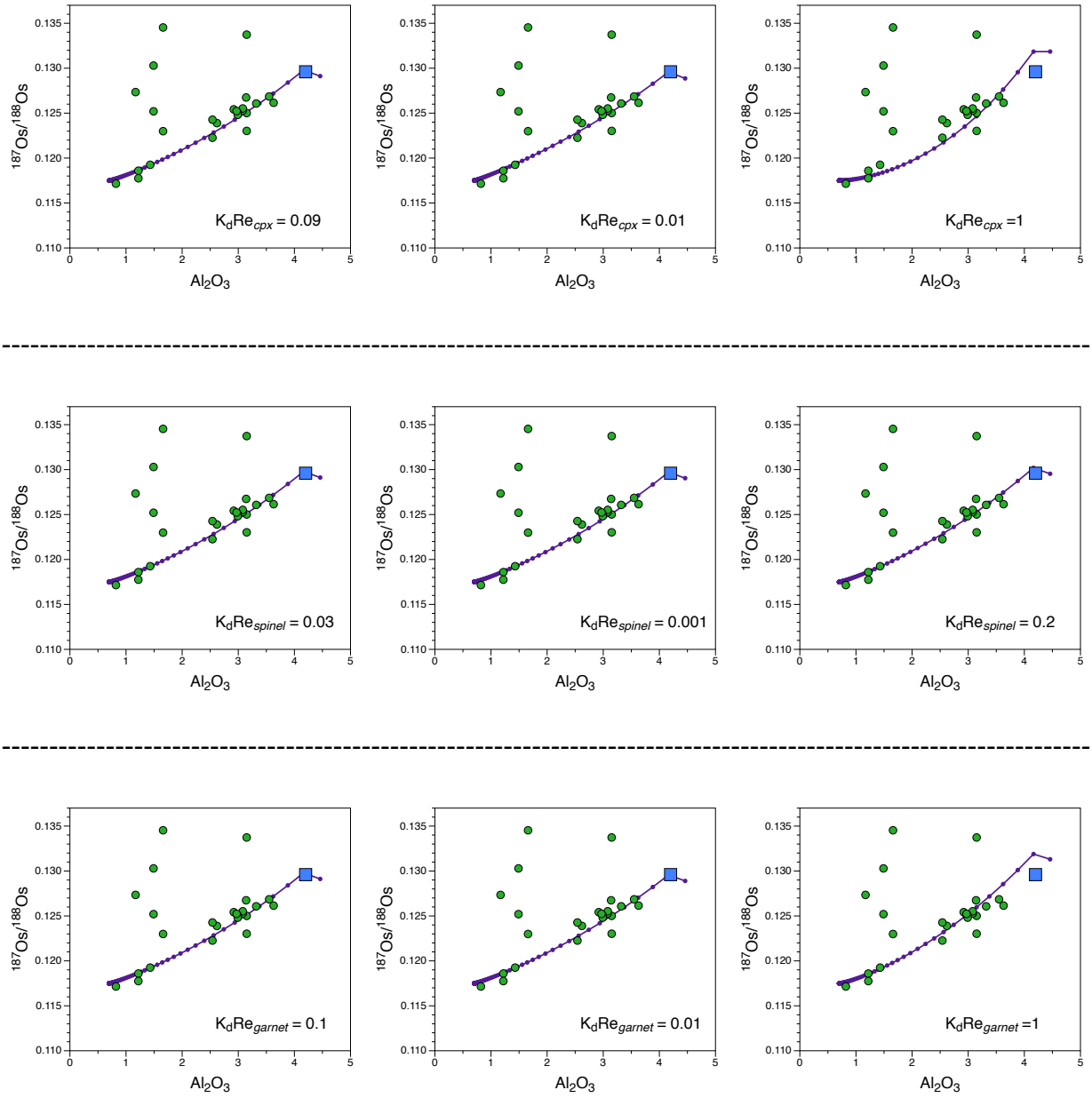

Effects of varying initial concentrations in peridotite and liquid

The [Os] of the liquid and the initial [Re] of the peridotite have very little effect of the model results. The initial [Os] of the peridotite, the [Re] of the liquid, and the Al_2O_3 content of the liquid have small to moderate effects.

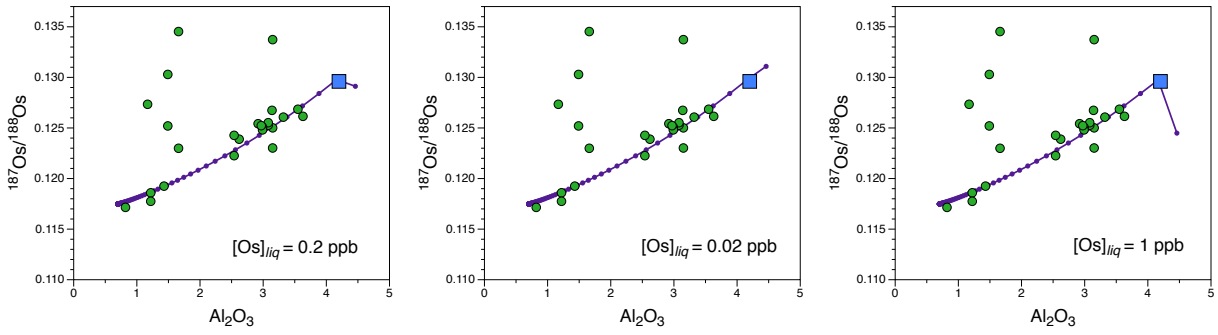

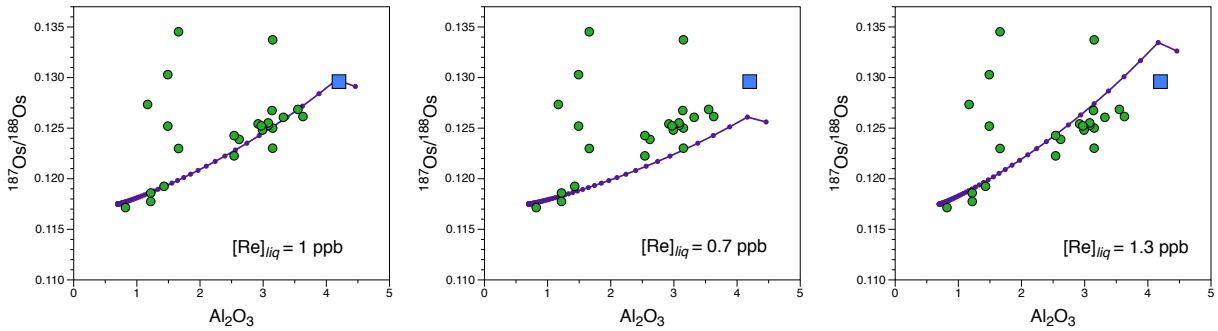
$^{187}Os/^{188}Os$
Al_2O_3
[Re]$_{liq}$ = 1 ppb
[Re]$_{liq}$ = 0.7 ppb
[Re]$_{liq}$ = 1.3 ppb

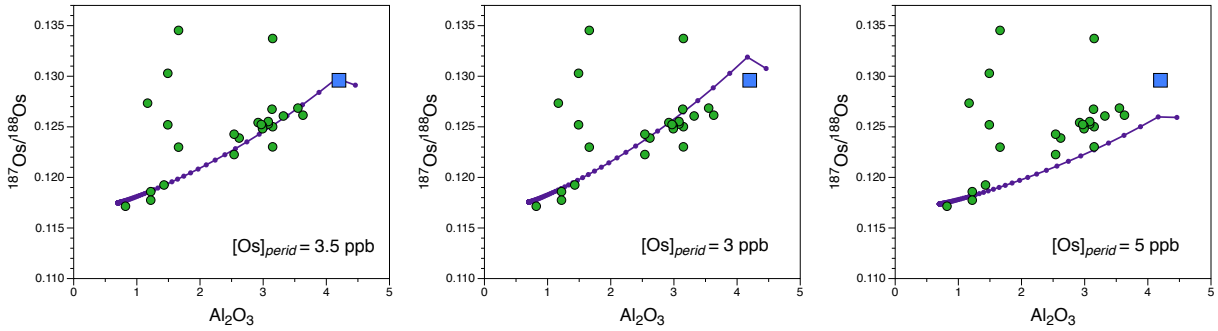
$^{187}Os/^{188}Os$
Al_2O_3
[Os]$_{perid}$ = 3.5 ppb
[Os]$_{perid}$ = 3 ppb
[Os]$_{perid}$ = 5 ppb

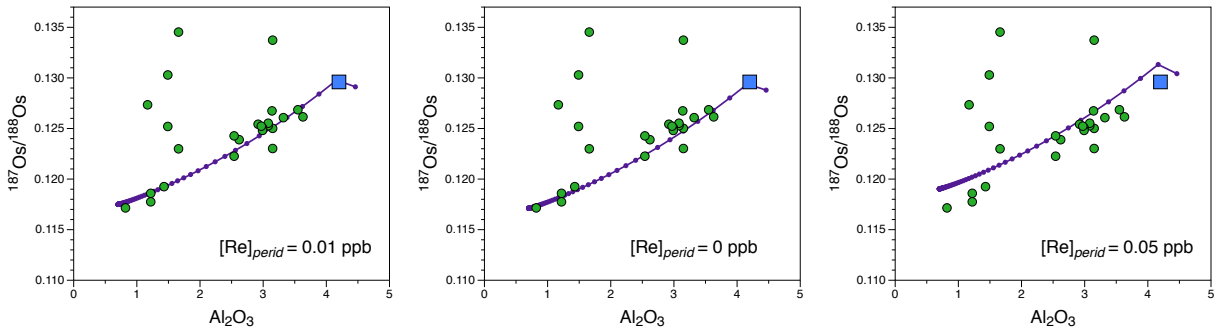
$^{187}Os/^{188}Os$
Al_2O_3
[Re]$_{perid}$ = 0.01 ppb
[Re]$_{perid}$ = 0 ppb
[Re]$_{perid}$ = 0.05 ppb

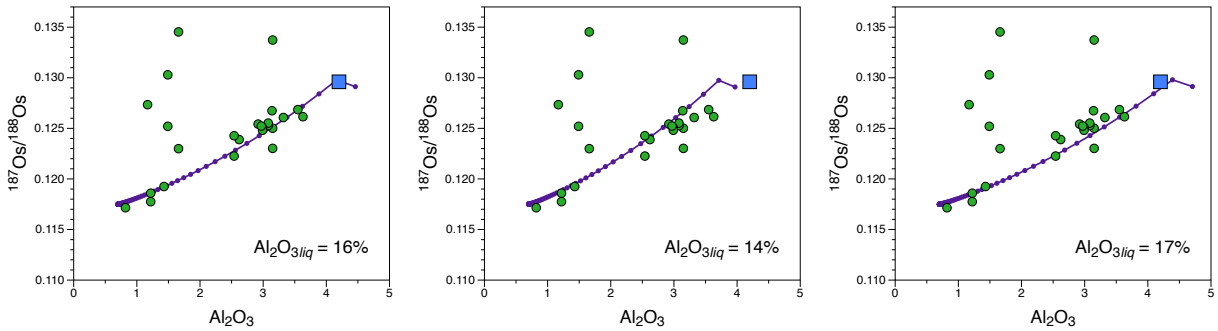
$^{187}Os/^{188}Os$
Al_2O_3
Al_2O_{3liq} = 16%
Al_2O_{3liq} = 14%
Al_2O_{3liq} = 17%

Parameters that influence the extent of the process

Like initial melt fraction (see main text), the crystallization fraction in each increment and the number of increments determine the extent to which the process proceeds, but have very little effect on the slope or the curvature.